

Determining the Sula block kinematics in the triple junction area in Indonesia by GPS

Andrea Walpersdorf,^{1,*} Christophe Vigny,¹ P. Manurung,² C. Subarya²
and S. Sutisna²

¹ *Ecole Normale Supérieure, Laboratoire de Géologie, Paris, France*

² *BAKOSURTANAL, Cibinong, Indonesia*

Accepted 1998 May 18. Received 1998 February 25; in original form 1997 October 1

SUMMARY

The point of convergence of the Eurasian, Philippine and Australian plates is situated adjacent to the island of Sulawesi, Indonesia. The relative plate velocities are estimated by NUVEL1 to be 7 to 9 cm yr⁻¹. The complex tectonic mechanism of the triple junction has been studied over a two-year period in the course of the GEODYSSSEA Southeast Asian Project. The GPS investigations concentrate on measurements of both the Sulawesi (eastern Indonesia) part of the inter-regional GEODYSSSEA network and a local subnetwork on Sulawesi. Motions derived using data from the subnetwork confirm what the results of the inter-regional GEODYSSSEA network have suggested; that is, that current deformation is high, and there are distinct deformation domains in the study area on Sulawesi. The tectonic mechanism of the triple junction has been analysed using a rigid microblock model. The triple junction area can best be interpreted as a headland of the Australian Plate deflected by its collision with the Philippine Plate, thereby identifying the driving forces of the current deformation. The northern part is dominated by the Sula domain, which shows clockwise rotation. To the south, it is connected to the Australian Plate by an ensemble of microblocks undergoing counter-clockwise rotation. In addition to the above, our tectonic model permits the determination of the local influence of two large earthquakes ($M=7.8$, 1996 January 1 and $M=7.0$, 1996 July 22) on the motion of the station Tomini (north Sulawesi). More observations and a denser GPS network are planned in order to study the behaviour of the Palu-Koro Fault, the main fault on the western limit of the Sula block.

Key words: Global Positioning System (GPS), Indonesia, Sulawesi, tectonics, triple junction.

1 INTRODUCTION

The GEODYSSSEA network in Southeast Asia covers the area adjoining the junction of the Eurasian, Philippine and Australian plates. The rigid plate kinematic model NUVEL1-A (DeMets *et al.* 1994) predicts very high relative velocities of 7.5 to 9.0 cm yr⁻¹ between the major plates and an apparent triple junction in eastern Indonesia (Fig. 1).

About 40 GEODYSSSEA GPS stations were installed and measured during two observation campaigns in December 1994 and April 1996 as part of the international project between the European Union and the ASEAN countries (Indonesia, Malaysia, Singapore, the Philippines, Thailand,

Vietnam and Brunei) (Wilson & Rais 1998). Comparing the solutions produced by four independent data processing centres, Angermann *et al.* (1998) showed that the observations are precise to about 5 mm yr⁻¹ on 1000 km baselines. In this paper those results from the GPS observations are presented that cover what is known as the most highly deforming area of the GEODYSSSEA network: the triple junction region between Sulawesi and the Moluccas in eastern Indonesia (Fig. 1).

According to NUVEL1-A, the triple junction is of trench–trench–(transform) fault (TTF) type, with the Australian and Philippine plates being subducted beneath the Eurasian Plate, and the Australian–Philippine boundary displaying left-lateral strike-slip faulting, with a small reverse component. A closer look at the tectonic features in the triple junction area (Fig. 1) shows that its mechanism is more complicated than the description above of the intersection of three simplified plate boundaries may imply.

* Now at: Delft Institute for Earth-Oriented Space Research, Delft University of Technology, Kluyverweg 1, 2629 HS Delft, the Netherlands. E-mail: andrea.walpersdorf@lr.tudelft.nl

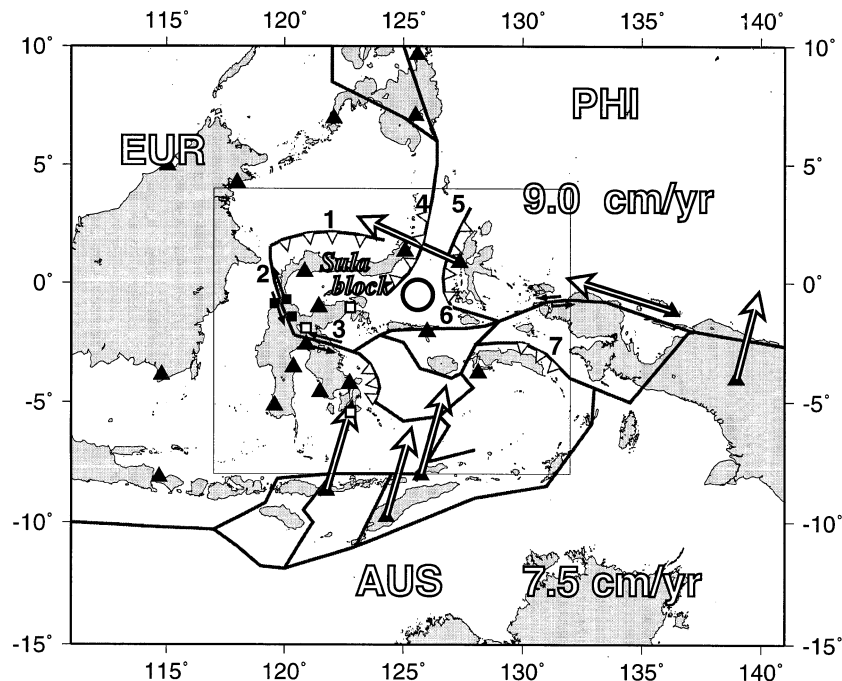


Figure 1. Tectonic setting of the Southeast Asian triple junction region and predicted motions of the major tectonic plates with respect to Eurasia according to NUVEL1-A (DeMets *et al.* 1994). Stations of the GEODYSSSEA network are indicated by triangles. Densification stations are shown by squares. All of these stations except those marked by open squares have been measured twice. The most important active tectonic features close to the triple junction area (inside the box) are (1) the North Sulawesi Trench, (2) the Palu-Koro Fault, (3) the Matano Fault, (4) the East Sangihe Fault, (5) the West Halmahera Trough, (6) the Sula-Sorong Fault and (7) the Seram Trough. Faults with teeth represent subduction zones (teeth on upper plate). The Sula block, a mainly rigid tectonic domain, is limited by features (1)–(3) to the north, west and southwest, whereas the eastern and southeastern boundaries are still uncertain. The intersection of the three major plates taking into account these observations is indicated by the circle in the Molucca Sea.

In the following, the tectonic mechanism is analysed in terms of rigid block rotations using a model based on the observed velocities. The model uses those rotation poles that fit the observed tectonic configuration and kinematics best, and evaluates the rates of rigid rotation. By examining the residuals between model and measured velocities, actively deforming areas are identified in detail. Furthermore, the model permits the estimation of the continuous secular motion of a station affected by earthquakes, thereby separating the coseismic displacements that help to constrain the earthquake mechanisms.

2 TECTONIC SETTING

The triple junction area between the island of Sulawesi and the Moluccas in eastern Indonesia shows a very complex tectonic scenario. Fig. 1 shows the tectonic features that are acknowledged to be active, based on Rangin *et al.* (1998), Rangin (1989), Hall *et al.* (1991), Silver, McCaffrey & Smith (1983) and Moore & Silver (1983). Instead of a simple intersection of three plate boundaries, one sees that the collision of the Philippine and Eurasian plates is absorbed by the double subduction zone in the Molucca Sea (features 4 and 5 in Fig. 1), for example. The Philippine and Australian plates are separated by the Sula Sorong Fault (feature 6) and the subduction zone north of Seram (7). The Sula block collides northwest of Sulawesi with the Eurasian Plate under the constraints of the Australian and Philippine plate motions.

This movement is transformed by the Matano Fault (3) and the Palu-Koro Fault (2) in central Sulawesi, and by the North Sulawesi Trench (1). A simplified best-fit location of the assumed triple junction is indicated by the circle located in the Molucca Sea. The analysis below of the observed velocities shows that the Sula domain is the dominant tectonic feature in the triple junction area.

3 GPS OBSERVATIONS

The GEODYSSSEA network, marked by triangles in Fig. 1, has been observed during two five-day campaigns of continuous simultaneous measurements—from 28 November to 2 December 1994 and 1.5 years later, from 18 to 22 April 1996. Six densification stations (indicated by open and filled squares in Fig. 1) have been measured during an additional session after the second GEODYSSSEA campaign in April 1996. The receivers operated in this part of the GEODYSSSEA network were Trimble SSE with SST and SSE antennas. Additionally, data from a local network in the Palu region at the end of September 1995 and in mid-December 1996 were used. In these campaigns some densification sites in the Palu region were reoccupied (filled squares in Fig. 1), and the latter campaign also includes the TOMI GEODYSSSEA site in northwest Sulawesi. These two campaigns have been carried out in collaboration with the Indonesian Survey and Mapping Agency (BAKOSURTANAL), Java, using their Ashtech Z12 receivers. We were able to derive the displacement of the

densification station TOBO using the result of an even longer observation period of the local Palu network (Walpersdorf *et al.* 1998).

In the following, we will refer to the four measurement epochs November–December 1994, September 1995, April 1996 and December 1996 as epochs 94, 95, 96.1 and 96.2.

In the analysis of the GPS data from the measurement campaigns described we included data from the five closest IGS stations, KIT3, TAIW, TIDB, TSKB and YAR1, and, when available, from the AUSLIG stations COCO, KARR, XMAS and DARW. The data acquired at a measurement interval of 30 s have not been decimated during the whole processing procedure. Precise IGS combined orbits were employed simultaneously with IERS Bulletin B Earth orientation parameters.

The processing software used are the MIT software packages GAMIT 9.4, GLOBK 4.0 and FONDA 1.1. The processing strategy applied for the ENS GEODYSSSEA solution is explained in detail in Angermann *et al.* (1998). The same approach was used for the processing of the two local measurement campaigns in the Palu region. In summary, the data processing was executed as following.

(1) First, for each of the measurement campaigns daily solutions were calculated in 24 hr sessions using GAMIT (King & Bock 1993). The observables were examined in an ionosphere-free combination (LC) and clock errors were eliminated by forming double differences. Tropospheric parameters were estimated every 3 hr for each station. The antenna phase centre variations were modelled using the tables recommended by IGS (Rothacher & Mader 1996). In the solution for each individual session the IGS orbits were kept fixed. Phase ambiguity resolution was attempted by a routine provided in Dong & Bock (1989).

(2) The scatter of independent results of the 24 hr sessions for each baseline component represented the repeatability of the measurement and gave an evaluation of its uncertainty.

During the first GEODYSSSEA campaign in 1994 (epoch 94), 11 stations in the local triple junction network were measured, most of them continuously, in five sessions of 24 hr. During GEODYSSSEA 1996 (epoch 96.1), 17 stations were observed in a sequence of three sessions of 5, 3 and 4 days. We obtained a mean repeatability of the solutions on this local part of the GEODYSSSEA network of 4–6 mm on the north, 5–7 mm on the east, and 15–17 mm on the vertical baseline components. The local Palu network measured in September 1995 (epoch 95) and December 1996 (epoch 96.2) includes two stations of the triple junction network of 1995 and four stations of 1996. The mean repeatabilities on these baselines are comparable to those of the main GEODYSSSEA results.

(3) Global campaign solutions were established using GLOBK, which is a Kalman filter applied to the analysis of solution vectors and associated covariance matrices generated during daily GAMIT solutions (Herring, Davis & Shapiro 1990). The GAMIT solutions passed to GLOBK are those with unconstrained station coordinates. The fixed orbit parameters in the daily solution are not re-estimated in the global solution.

The velocity solution is obtained by combining the different epochs. The displacements over the interval of 17 months between the two GEODYSSSEA measurement campaigns is attributed to a linear velocity of each of the GEODYSSSEA stations. The combination of the measurement epochs 95, 96.1

(GEODYSSSEA 1996) and 96.2 establishes the velocities of three densification stations (WATA, TOBO, WUAS) and a second displacement rate for the TOMI station that has already been observed in both of the GEODYSSSEA campaigns.

(4) The network adjustment program FONDA developed at MIT and JPL (Dong 1993) is used to calculate the distribution of strain and spin in the network (Feigl, King & Jordan 1990). Input data for this was the station coordinates and velocities from the free network GLOBK solution. The representation in terms of deformation is independent of the reference frame chosen for the velocities. The TOMI station clearly showed coseismic displacements and was excluded from the study of the continuous strain and spin field. The limit of strain resolution in the GEODYSSSEA network is estimated to be 6 mm yr^{-1} on 1000 km baseline lengths (6 ppb yr^{-1}) by comparing individual solutions and the combined GEODYSSSEA solution. This value is in good agreement with the estimation of Angermann *et al.* (1998) (see above), and can be considered as a realistic value for the velocity uncertainties.

The high quality of these GPS measurements is further supported by (1) the careful choice of GEODYSSSEA GPS sites (mainly in outcrops of substratum) and (2) the use of screw markers, where the antennas are directly screwed on (there is no error source from an inadequately installed tripod; in this way the remeasurement of exactly the same point is guaranteed). This means that the observed displacements are not due to operation errors or local site instabilities, but are caused by tectonics and minor error sources (e.g. errors due to varying weather conditions).

However, we cannot account for the possible effects of time-correlated errors on the accuracy of our velocity field. Since their amplitude is small compared to the tectonic signal obtained here, we assume that time-correlated errors will not affect our main conclusions.

4 THE VELOCITY FIELD

The velocity field in the triple junction region obtained by the two GEODYSSSEA measurement campaigns is presented in Fig. 2. In the chosen reference frame the South China Sea is held fixed by minimizing the velocities of three GEODYSSSEA stations situated adjacent to the South China Sea [Tanjung Bajau (West Kalimantan), Non Nuoc (Vietnam), Kuala Trengganu (Malaysia)]. The mean residual velocity for these three stations is 1.7 mm yr^{-1} , far below the measurement uncertainties, so that the representation of the velocities is realized in a coherent way. The choice of the South China Sea as a reference frame is appropriate since this region forms the approximate centre of the large rigid block known as Sundaland. This rigid block has only recently been detected, and its movement, which is independent of and slightly different from that of Eurasia, has been deduced from observations on the GEODYSSSEA network (Chamot-Rooke *et al.* 1998). Its rigidity is demonstrated by the low residuals ($1\text{--}2 \text{ mm yr}^{-1}$) of the velocity observations with respect to modelled velocity according to rigid rotation around the best-fitting rotation pole (situated south of Australia in a Eurasian reference frame). Tregoning *et al.* (1994) presented geodetic observations that show that the motion of the southern part of Sundaland, with respect to Australia, is already different from Eurasian Plate motion according to NUVEL1-A.

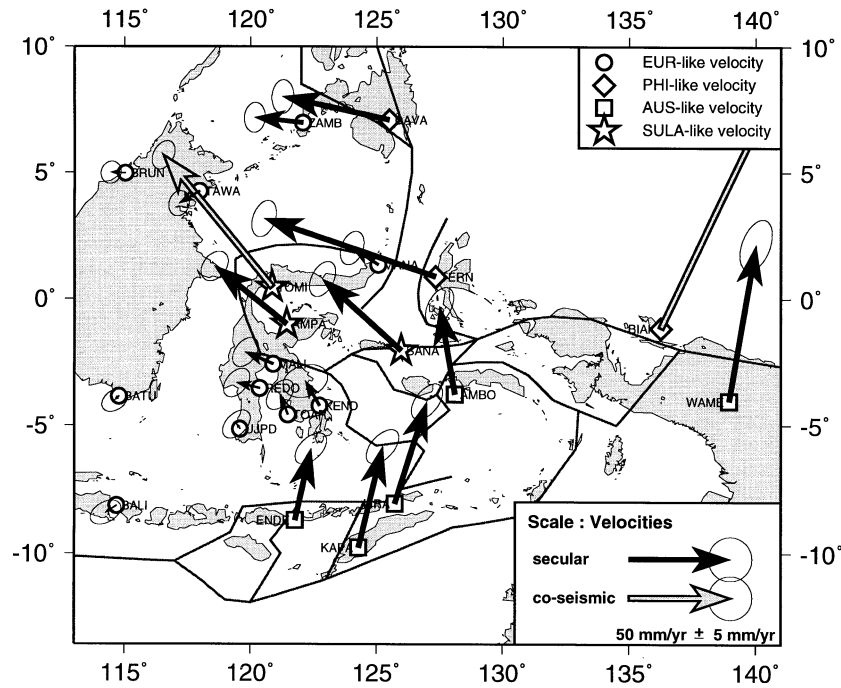


Figure 2. GEODYSSSEA velocities in the triple junction area. Reference frame is with respect to the South China Sea held fixed. The station velocities are attributed to one of the major tectonic plates as shown by the different symbols at the station locations, except for stations in the Sula domain, with displacements clearly different from EUR-, AUS- or PHI-like velocities. The error ellipses indicate a formal uncertainty of 1σ . A realistic error of the measured velocities is estimated as about 6 mm yr^{-1} .

The southwesternmost part of Sulawesi is included in Sundaland. Therefore, in the chosen reference frame, the southern part of Sulawesi has a very slow motion (the residuals resulting from a small amount of deformation in the Makassar Strait or from elastic strain accumulated along the Palu-Matano Fault Zone), so differential velocities in the local network can easily be observed. The numerical values of the velocities in this reference frame are given in Table 1.

Two stations in the triple junction region, TOMI and BIAK (light grey vectors in Fig. 2, BIAK exceeding the figure limits) suffered a large earthquake close to the site between the two GEODYSSSEA measurement campaigns. Their displacement rates include apparent co- and post-seismic displacements, so that they are not representative of secular tectonic velocities. Estimations of the seismic displacement due to the February 1996 earthquake from a GPS station close to GEODYSSSEA's BIAK site are given by McCaffrey *et al.* (1996) based on their measurements of the station velocity from 1991 to 1993. A last occupation in March 1996, following the earthquake, provided these authors with a BIAK displacement that shows the same direction as, but a smaller magnitude than, the GEODYSSSEA results. We suggest that the GEODYSSSEA solution includes post-seismic deformation that was not detected by McCaffrey.

The other observed velocities in the triple junction area coincide in most cases with the NUVEL1-A predictions for one of the three major plates: low velocities in the western part of Fig. 2 are compatible with the motion of Sundaland (these stations are indicated by circles in Fig. 2), westward velocities in the northeast with Philippine Plate motion (stations shown by diamonds) and northeastward velocities in the south with Australian Plate motion (stations shown by squares).

Table 1. Horizontal site velocities with 1σ uncertainties and north to east correlation coefficients derived from GPS campaigns GEODYSSSEA 1994 and 1996.

Site Code	Latitude °N	Longitude °E	Velocities (mm yr^{-1})		N-E correlation
			north	east	
AMBO	-3.7500	128.1169	43 ± 4	-8 ± 3	0.46
AMPA	-1.0032	121.4362	28 ± 3	-36 ± 3	0.34
BALI	-8.0936	114.6800	-3 ± 3	-5 ± 4	0.40
BATU	-3.8414	114.7912	-2 ± 3	-2 ± 3	0.36
BRUN	4.9332	115.0309	0 ± 3	-7 ± 2	0.09
DAVA	7.0372	125.5081	12 ± 4	-53 ± 3	0.08
ENDE	-8.6496	121.7657	35 ± 4	8 ± 4	0.51
KAPA	-9.7121	124.2804	49 ± 4	12 ± 4	0.54
KEND	-4.1985	122.7362	12 ± 4	-7 ± 5	0.23
LIRA	-8.0058	125.7387	50 ± 4	16 ± 4	0.52
MALI	-2.5776	120.9048	6 ± 3	-14 ± 3	0.41
MANA	1.3220	125.0637	8 ± 4	-13 ± 3	0.32
REDO	-3.5158	120.3674	3 ± 3	-11 ± 3	0.43
SANA	-2.0347	125.9910	35 ± 4	-39 ± 3	0.42
TAWA	4.2230	117.9786	-6 ± 3	-10 ± 2	0.16
TERN	0.8546	127.3417	29 ± 4	-85 ± 3	0.34
TOAR	-4.5513	121.4895	10 ± 3	-4 ± 3	0.46
UJPD	-5.1194	119.5810	2 ± 3	-2 ± 3	0.45
WAME	-4.0149	138.9521	77 ± 6	13 ± 4	0.42
ZAMB	6.9264	122.0728	3 ± 3	-24 ± 2	0.06
KUAL ¹	5.2835	103.1392	2 ± 1	0 ± 2	0.02
NONN ¹	15.9020	108.2634	-4 ± 2	-1 ± 1	0.25
TABA ¹	0.8570	108.8909	-2 ± 2	1 ± 1	-0.15
BIAK ²	-1.1596	136.2483	916 ± 5	437 ± 3	0.37
TOMI ²	0.4501	120.8499	65 ± 3	-54 ± 3	0.34

¹ South China Sea stations with minimized velocities.

² Earthquake-affected stations.

Except for the slight differences from the principal motion in south Sulawesi noted above, some other small variations are observed. An increase from north to south of the westward velocity of the Philippine Plate (DAVA and TERN in Fig. 2) is related to the rotation of this plate around a pole situated further north and to the absorption of part of the Philippine Plate motion by the Philippine Trench east of DAVA. Nonetheless, the observed TERN displacement rate is about 1 cm yr^{-1} slower in the western direction than the NUVEL1-A prediction of Philippine Plate motion at this location. This difference might be due to accumulated interseismic strain close to the subduction zone in the Molucca Sea.

For the Australian Plate, the station velocities on Timor and Flores show that a minor fraction of the original motion is absorbed in the Java Trench or by short-term elastic strain on transform faults close to ENDE, for example. This seems to be confirmed by a comparison with GPS velocities in the Banda arc observed by Genrich *et al.* (1996). In general, our displacement rates for KAPA, LIRA and ENDE on Timor, Liran Island (southeast of Wetar Island) and Flores in the South China Sea reference frame are about 1 cm yr^{-1} slower on the north component and directed more to the east than the observations of Genrich *et al.* (1996) for KUPA (Timor), WETA (Wetar Island) and MAUM (Flores) with respect to a fixed Sunda Shelf. The only deviation from this trend is seen when ENDE is compared to MAUM: the difference on the north component is more than 2 cm yr^{-1} . ENDE is situated closer to the fault zone in central Flores than MAUM, and seems to be affected by the elastic strain field surrounding this active fault. AMBO motion to the NNW rather than the NNE, like the Australian Plate in the same reference frame (Fig. 2), shows interaction with Philippine motion, although the station is situated south of the Seram Trough and therefore is clearly separated from the Philippine Plate. Finally, the similar velocities of the stations AMPA and SANA, which are situated in the Sula domain (defined in Fig. 1), are clearly different from any of the major plate velocities. The velocity of AMPA and SANA appears to be a combination of the Australian and Philippine plate velocities. This implies that the Sula domain could be a slightly rotated and slower-moving headland of the Philippine Plate, or a highly deflected headland of the Australian Plate. The major boundary between the Philippine Plate and the Australian Plate to the east of the triple junction was for a long time considered to be the Sorong Fault. However, Puntodewo *et al.* (1994) showed that the Sorong Fault displays no major activity in Irian Jaya. Interaction with Philippine Plate motion south of the Sorong Fault is compatible with the still clearly westward motion of the station SANA, which is situated just to the south of the western extension of the Sorong Fault in our triple junction network.

The major aim of this study is to use our GPS observations for determining both the driving forces of the kinematics of the Sula domain, and the location of the block limits with respect to the Philippine and Australian plates.

The assumption that Sula is a deflected headland of Australia is emphasized by the amplitudes of the Sula block velocities, which are similar to those of the Australian Plate, but with varying directions, implying deflection and distributed deformation in the zone relating the Sula domain to the Australian Plate. Geological and geodetic evidence for this hypothesis could be given by the accretion of the southern Banda arc to the Australian Plate margin (Genrich *et al.* 1996),

for example, indicating the extension to the north of the zone with characteristic Australian Plate motion. Furthermore, a large number of microblocks (e.g. the Buru block, the North Banda Basin and the Banda block) and active faults exist in the Banda Sea region (Rangin *et al.* 1998), and a deformation zone in the South Banda Sea is suggested by McCaffrey & Abers (1991), all of these phenomena accommodating the high deflection of the Sula domain motion with respect to Australian Plate motion.

The other hypothesis, that the Sula domain is a headland of the Philippine Plate, is supported by the common direction of motion of the AMPA and SANA velocities and the Philippine Plate. In this case the Sula domain should be clearly limited to the south by an active block boundary, and its rotation should be related to the rotation of the Philippine Plate. However, according to our data, the Sula block moves more slowly to the NW than the Philippine Plate. This relative motion must be accommodated by an active block limit between the Philippine Plate and the Sula domain, which could be realized in this case of parallel displacements by strike-slip faulting along the North Sula Sorong Fault, for example, or by continuous deformation in a larger transition area. An argument in favour of this hypothesis is provided by Puntodewo *et al.* (1994). They show that at the same latitude as the Sula domain, but further east, the forces driving the deformation are related to the motion of the Pacific Plate (which is similar to Philippine Plate motion), not to the motion of the Australian Plate. Puntodewo *et al.* (1994) show typical Pacific-like motions for a station south of the Sorong Fault, and suggest that the major active limit with respect to the Australian Plate is found in the Birds Neck Belt, rather than in the Sorong Fault as is commonly suggested.

The two hypotheses have different consequences for the location of the intersection of the three simplified plate boundaries between the Eurasian, Philippine and Australian plates. For the Australian Plate extending into the Sula domain, this assumed triple junction is found in the Molucca Sea, consistent with the tectonic observations (Fig. 1). The plate limits in the case of the Sula domain being kinematically part of the Philippine Plate show an intersection in the Banda Sea southeast of Sulawesi, which would result in the location of the triple junction being about 800 km south of that in the first model. Furthermore, the kinematic relation of the Sula domain to one of the two major tectonic plates determines the present-day status of the time evolution of the triple junction zone. Geologically, the North Banda Sea and the Sula Islands are of Australian origin and part of east Sulawesi has Australian affinities (Rangin *et al.* 1990). Evaluating how much the Sula domain motion is currently constrained by the Philippine Plate or by the Australian Plate will indicate the progress of accretion and the present state of the tectonic evolution of the triple junction area.

According to the existing velocity observations, either of these Sula domain models (direction of motion consistent with the Philippine Plate or the deflection of the Sula block relating it to the Australian Plate) might be a consequence of deflection of the Australian Plate as a result of its collision with the Philippine Plate.

5 STRAIN AND SPIN DISTRIBUTION

One approach to regional kinematics has been to emphasize the major faults or boundaries and approximate the behaviour

of the area between the faults as rigid (Peltzer & Saucier 1996). This has been done by applying a rigid microblock model as shown in the next section. Another approach is to treat the deformation as being continuous but heterogeneous. Both approaches have their drawbacks: neither is the studied area between faults free of deformation, nor are the investigated faults and boundaries of considerably smaller dimensions than the deformed region. A major part of the deformation is accommodated along boundary faults.

The continuous approach has been applied to the study area using Delaunay triangles and triplets of nearest stations (Feigl *et al.* 1990). Results are 2-D principal strain or stretching axes and a specific amount of spin for each of the triangles. Thanks to the localizations of the GEODYSSSEA GPS stations with roughly one station per tectonic (micro-) block, we obtained significant strain and spin in nearly each Delaunay triangle in the triple junction area. The numerical values are strongly dependent on the triangles' geometries and should be considered only as a relative evaluation beneath the different triangles.

The major features of the distribution of horizontal deformation in the triple junction area are shown in Fig. 3(a). The major principal strains calculated from the Delaunay triangles indicate that stations AMPA and SANA on the Sula block, as well as the southern part of the Philippine Plate, are under compression, whereas extension dominates to the south. Fig. 3(a) shows these two zones as belts. Typical values are $-0.29 \mu\text{strain yr}^{-1}$ for the observed compression in the Molucca Sea, and $0.07 \mu\text{strain yr}^{-1}$ for the extension in the southern belt. This strain distribution suggests that the Sula domain deformation belongs to that of the southern Philippine Plate. A zone of extension separates the Sula domain–Southern Philippine assembly from Australia.

Spin rates derived in the triple junction area (Fig. 3b) indicate counter-clockwise rotation in southern Sulawesi and clockwise rotation in the northern part of Sulawesi. Typical values for the rotations within the chosen triangles are $3\text{--}4 \mu\text{rad yr}^{-1}$ for the clockwise rotation in northern Sulawesi and $5\text{--}10 \mu\text{rad yr}^{-1}$ for the counter-clockwise rotation in southern Sulawesi.

6 MODELLING

Geological evidence for the clockwise apparently rigid microblock rotation in northern Sulawesi, with a rotation pole close to Manado in northeast Sulawesi, is given by Silver *et al.* (1983), Surmont *et al.* (1994) and Rangin *et al.* (1997). Most of the Sula/Sunda deformation is accommodated along the Palu-Koro and Matano faults in central Sulawesi. These faults form a small circle around an assumed rotation pole in the area of Manado (Fig. 1).

To obtain quantitative estimates of the rates of clockwise rotation in northern Sulawesi from our observations, we apply a model of rigid microblock rotations in order to describe the measured velocities. This strategy might provide further insight into the deformation in the block or plate transition zones or the internal deformation of the tectonic domains themselves if the residuals between the rigid block model and the observed displacement rates are studied. The model which best explains the measurements in the triple junction area comprises two rotation poles with opposite signs, as shown in Fig. 4.

The clockwise rotation of the northern part of Sulawesi is constrained best by the MANA, AMPA, WUAS and TOBO velocities, determining the pole P1 northeast of Sulawesi at 2.2°N , 126.2°E with a clockwise rotation rate of $3.4^\circ \text{Myr}^{-1}$ in the South China Sea reference frame. The TOMI motion is not included in the estimation, as this station was affected by two large earthquakes. We observe that the rigid block model shows smaller residuals for the MANA and AMPA stations, and larger residuals for TOBO and WUAS, thus the first two stations represent the motion of the apparently more rigid part of the tectonic block. The displacement of the latter two sites might be affected by deformation processes along the block boundaries, suggesting that this deformation occurs in a large zone several tens of kilometres wide.

For the station TOBO two displacement rates were derived. The higher rate was observed from September 1995 to December 1996, and the smaller rate was deduced from a longer observation series on the subnetwork commencing in 1992 (Stevens *et al.* 1998; Walpersdorf *et al.* 1998). The higher observed rate and the direction of deflection of the TOBO motion seems to indicate that TOBO has suffered a seismic displacement related to the earthquake of 1996 January 1 northwest of TOMI on the North Sulawesi Trench. The rate trends converge over a longer time-span towards the station velocity predicted by our time-invariant model, although the direction of motion is still deflected. The secular displacement rate of WUAS, situated 100 km south of TOBO, is probably affected by the elastic strain caused by the nearby (30 km) locked Palu Fault. This suggests that discontinuous deformation occurs adjacent to the Palu Fault and may even be related to the North Sulawesi Trench over 150 km away.

In the modelling, the parallel AMPA and SANA velocities cannot be described as a common rotation around a pole in the MANA region. Therefore, SANA seems to be situated outside the Sula block, whose southeastern limit consequently must pass northwest of SANA, as indicated in Fig. 4. An attempt to model SANA together with the stations further south provided better results, indicating a kinematic connection between the Sula block and the Australian Plate. A second pole, P2, of counter-clockwise rotation for southern Sulawesi at 4.7°S , 123.8°E with a rotation rate of $6.0^\circ \text{Myr}^{-1}$ in the South China Sea reference frame, constrained by the SANA and AMBO velocities, shows low residuals. When including the closest stations on the Australian Plate in the computation, a coherent counter-clockwise rotation with AMBO still results in higher residuals for SANA. This implies a highly deforming zone south of the Sula domain, or the presence of more rigid microblocks separated by active block limits.

The high residuals do not preclude the use of the rigid rotation model, as we have applied this model intentionally for regions that are partially deformed and where only very few velocities are known in the rigid parts. High residuals are to be expected; they provide a means to emphasize the observation of deformation, rather than being a sign of a deficiency in the model.

The pole parameters (latitude, longitude and rotation rate) were evaluated by a least-squares method; the 1σ standard deviations are indicated in Fig. 4 by ellipses around their mean position. The well-constrained positions of the two poles show that the model chosen is an appropriate way of describing the kinematics of the area. The corresponding variations of the modelled velocities are indicated by error ellipses around the vector heads.

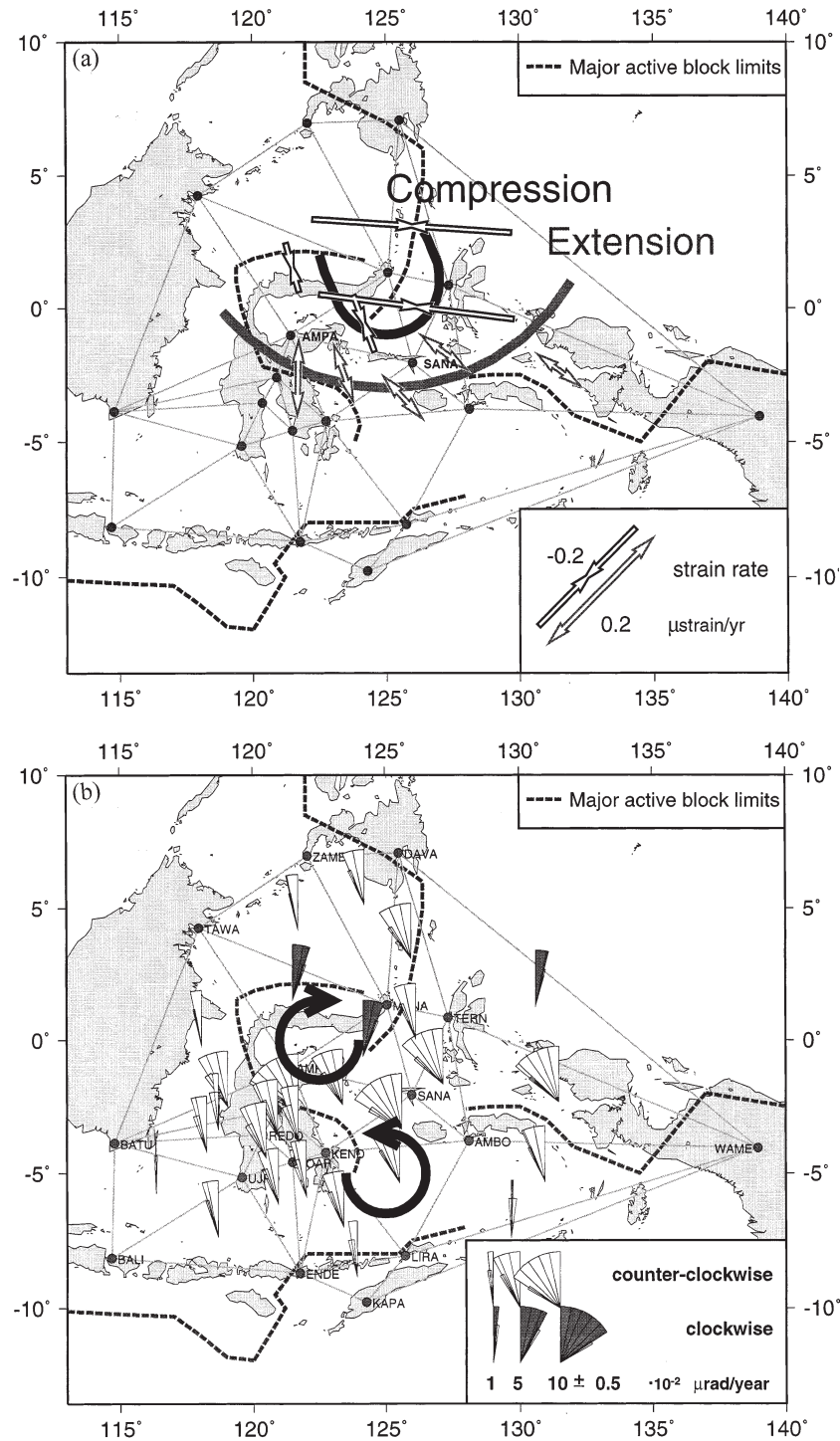


Figure 3. (a) Dominant features of the strain distribution in the triple junction area: compression connecting the Sula block to the Philippine Plate, extension separating the Sula block from the Australian Plate. (b) Distribution of spin, showing two rotations with opposite signs in north and south Sulawesi.

Other models have been tested that lead to slightly higher average residuals than those given by the chosen model. With the residuals being of only limited use in choosing a model, independent geological and geodynamic information has been used to determine the most appropriate solution. Moreover, we preferred the model constrained by the highest number of observed velocities. The model with the second-lowest

residuals was obtained by excluding MANA when constraining the pole P1, because MANA might not be situated on the same rigid block as AMPA, TOBO and WUAS. This would invalidate our assumption that the northern arm of Sulawesi shows no active deformation at present. The TOBO and WUAS velocities in the deformed Palu Fault area are given a higher weight in constraining the pole, which is found

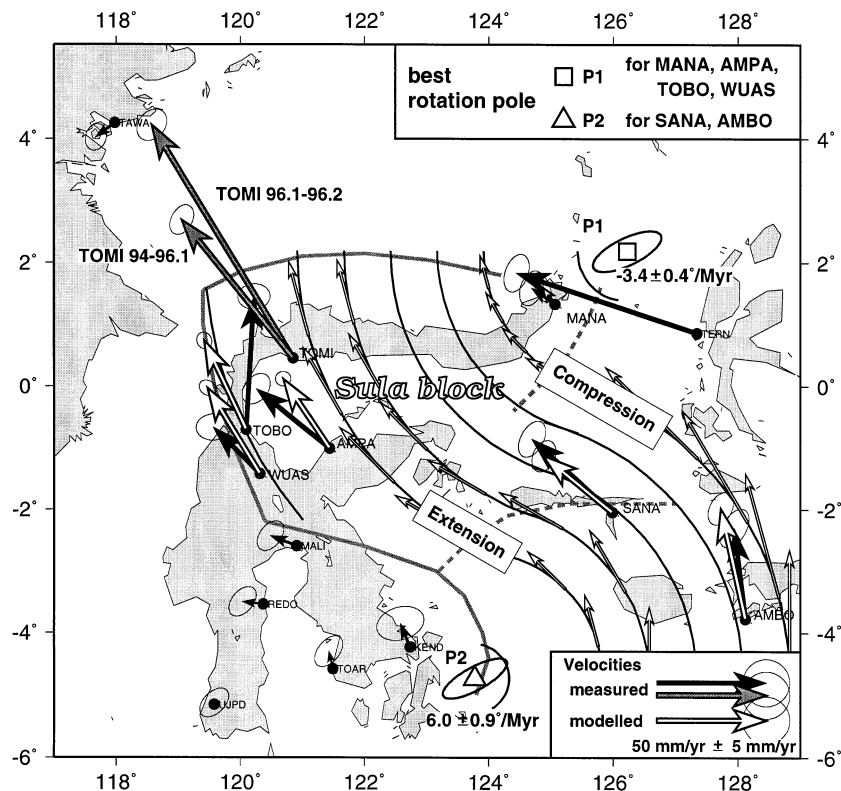


Figure 4. Model of two rotation poles describing the kinematics in the triple junction area. Velocities inferred by the two GEODYSSSEA campaigns (epochs 94 and 96.1) and by the December 1996 campaign (epoch 96.2) indicate $3.4^\circ \text{ Myr}^{-1}$ clockwise rotation for P1 and $6.0^\circ \text{ Myr}^{-1}$ counter clockwise rotation for P2 with respect to a fixed South China Sea. The best pole locations and their 1σ standard deviations (shown by the ellipses around the best locations) are computed by an iterative linear least-squares method. The suggested southeastern and eastern limits of the Sula block are schematically indicated by the dashed line. The two-pole geometry implies two zones of deformation (compression and extension) where areas of slow velocities close to one pole encounter areas of fast velocities created by the other, more distant pole.

to be significantly closer to the three remaining stations in the model. Until new velocity observations can distinguish between the best and the second-best models, preference is given here to the model including MANA in the determination of P1, as this involves the highest number of velocities. Moreover, the hypothesis that MANA is situated on the same microblock as AMPA, TOBO and WUAS is supported by geological studies (Silver *et al.* 1983; Surmont *et al.* 1994; Rangin *et al.* 1997).

The two-pole model with P1 and P2 computed from the displacement rates presently available has a number of characteristic features, and its agreement with geological and geodynamic observations shows that it is an appropriate way of describing the present-day tectonics of the triple junction area.

(1) The clockwise rotation rate with respect to the South China Sea obtained for P1 is $3.4 \pm 0.4^\circ \text{ Myr}^{-1}$. This value is in good agreement with mean rotation rates of geological models such as the model of Silver *et al.* (1983), which predicts about 4° Myr^{-1} with respect to a pole situated slightly closer to the northern arm than in our model.

(2) Comparing the Palu-Koro Fault system to a circle around the P1 rotation pole, purely strike-slip motion is implied in the TOBO region, extension further north and compression further south. Consistent with this, the observed TOBO velocity from 92 to 96.2 is parallel to the fault, with a tendency towards extension since 1995 (shown in Fig. 4 by the

longer, more northward TOBO vector), whereas the WUAS velocity shows a compressive component with respect to the Palu-Koro Fault.

(3) The AMBO and SANA displacements constrain the P2 pole of counter-clockwise rotation located in southern Sulawesi to a rotation rate of $6.0 \pm 0.9^\circ \text{ Myr}^{-1}$ with respect to a fixed South China Sea.

(4) The characteristic velocity field resulting from the two rotation poles is shown schematically in Fig. 4. The two-pole geometry implies the existence of a line of continuous displacement at the same velocity from SE to NW (line in Fig. 4 where modelled velocities have equal amplitude). To the NE of this line are lines of continuous motion, where deceleration takes place when passing from the domain of motion according to pole P2 into the domain of pole P1. On lines to the SW of that with equal velocity, acceleration takes place. Therefore, the two-pole geometry implies two special regions of deformation along the boundary between the two domains: a zone of extension is predicted in the southern part of the region between the two poles, and a zone of convergence further north, in the Molucca Sea. The corresponding velocity differences along the lines of continuous displacement can be evaluated at the positions of the 'extension' and 'compression' boxes in Fig. 4: there is an increase of 1 cm yr^{-1} in the extension zone, and a decrease of $3\text{--}4 \text{ cm yr}^{-1}$ in the compression zone. Both results are supported by the strain pattern and geological evidence found in the field. The extension rate of

1 cm yr^{-1} in the south is compatible with the fact that the Matano Fault shows a slower left-lateral strike-slip motion (about 2 cm yr^{-1} ; Silver *et al.* 1983) than the Palu-Koro Fault (over 3 cm yr^{-1} according to several studies). The convergence rate of $3\text{--}4 \text{ cm yr}^{-1}$ in the north is apparently absorbed by the double subduction zone in the Molucca Sea, and to some extent by the Seram Trough.

Even with the limited number of velocity observations in the triple junction, this model can be used to evaluate the present-day rate of clockwise rotation of the Sula block, which is in good agreement with the values obtained from geological studies for intervals of several million years. According to our model, the southeastern limit of the Sula block seems to pass north of SANA, indicating the Sula-Sorong Fault as the block boundary. The suggested schematical Sula block limits are displayed in Fig. 4. The velocity observations south of this fault (SANA and AMBO) have been described by the rotation pole P2, which shows the general motion pattern in the southern triple junction region and predicts a characteristic distribution of deformation along the southeastern Sula block boundary. Nevertheless, the rotation pole P2 cannot model the kinematics of the various microblocks and therefore cannot predict the tectonic activity along these microblock boundaries. The entire model will be better constrained by the measurements of densification points planned for the triple junction area.

7 TOMI DISPLACEMENT

The tectonic model could be better constrained by knowledge of the stationary velocity of the TOMI station. Unfortunately, between each of the three measurement campaigns on this site, a large earthquake occurred close to the station and superposed an instantaneous seismic displacement onto the secular velocity. The observed displacement rates are indicated in Fig. 4. The first large earthquake occurred at a point 130 km

WNW of TOMI on 1996 January 1 with a magnitude $M_s = 7.9$. A second earthquake, 70 km distant, took place on 1996 July 22, with $M_s = 7.0$. The modelling of the seismic displacements caused by these earthquakes has not yet been completed, so that the non-seismic velocity cannot yet be retrieved to constrain the modelling of the tectonic mechanism in the triple junction zone. Instead, we can use the model to give an estimation of the stationary velocity of station TOMI, using the assumptions that TOMI is situated on the same rigid block as stations AMPA, WUAS, TOBO and MANA and rotates with respect to the same pole northeast of Sulawesi. This velocity is indicated in Fig. 5, and it allows us to decompose the observed displacement rates from December 1994 to April 1996 and from April to December 1996 into a secular part and two instantaneous displacements caused by the two earthquakes (shown by grey vectors in Fig. 5). The azimuth of the slip vectors obtained using this model is about -50° . This is consistent with the alignment of aftershocks of the January 1996 earthquake (grey dots in Fig. 5), which indicate a rupture-zone azimuth of about 40° . Furthermore, these observations correspond to the tectonic model established by Rangin (1989), in which the Sula block moves in a NW direction and collides with the Sunda block. This motion is transformed at the western boundary of the Sula block by the Palu-Koro left-lateral strike-slip fault and is absorbed to the north at the North Sulawesi Trench. At the intersection of these two tectonic features, active thrust zones are formed that have azimuths of 40° . These thrust zones appear to be responsible for the observed earthquakes.

8 CONCLUSIONS AND PERSPECTIVES

The triple junction is not a simple intersection of three continuous plate boundaries, but rather consists of a transition zone that includes the Sula domain, which both transforms and accommodates the high differential motions of the Australian,

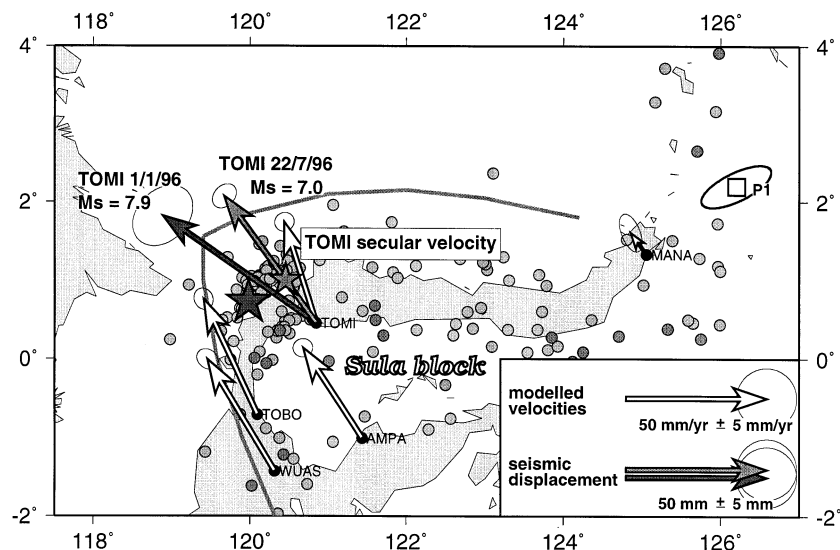


Figure 5. Continuous velocity for the station TOMI, modelled and constrained to a rigid rotation with respect to the rotation pole northeast of Sulawesi. The observed TOMI displacement rates shown in Fig. 4 are here decomposed into the secular velocity (in mm yr^{-1}) and the two instantaneous seismic displacements indicated, marked by grey vectors (in mm). These are related to the two seismic events shown by the stars. Further earthquakes (IRIS data) are indicated by circles, aligning the rupture zone along an azimuth of about 40° .

Philippine and Eurasian Plates. The dominant characteristic of this microblock is a velocity that differs from that of the Philippine and Australian plates. It can best be interpreted as a deflection of a headland of the Australian Plate in collision with the Philippine Plate. This identification of the driving forces of the current deformation is one of the main results of this study. Large amounts of deformation at the limits of the Sula domain have been shown by the application of a simple model in terms of rigid rotations. A model consisting of two rotation poles with opposing rotational sense (a clockwise rotation of $-3.4^\circ \text{ Myr}^{-1}$ in northern Sulawesi and a counter-clockwise rotation of 6° Myr^{-1} in southern Sulawesi with respect to a fixed South China Sea) (1) fits the observed velocities well, (2) indicates zones of distinct strain, and (3) is in good agreement with geological and tectonic observations in the area. This model has been applied in order to analyse coseismic displacements of the north Sulawesi station TOMI. It helps to constrain the earthquake mechanisms and serves to emphasize local tectonic features. For most of the stations in the triple junction area the velocities are deduced from only two measurement campaigns. A third measurement campaign will show which of the station velocities can be approximated by a rigid block model, continuous deformation or deformation along the major faults and subduction zones.

Precise plans for future measurements have been made to constrain the tectonic mechanism of the triple junction. The most promising project will be the remeasurement of the stations LUWU and KAMB, which have already been measured during the GEODYSSSEA 1996 campaign (open squares in Fig. 1). The next occupation of these sites will establish two new velocity vectors within the Sula domain. This will facilitate the distinction between zones of deformation along block boundaries and rigid microblock motion in the triple junction area. The western limit of the Sula domain is defined by the Palu-Koro Fault, a major transform zone displaying the high relative motions between the three major tectonic plates in the triple junction area. Seismic (elastic) loading is currently inferred for the Palu transect (6.3 cm yr^{-1} left-lateral strike-slip since 1995 instead of a 3.4 cm yr^{-1} average over 4.5 yr). This can be related to the seismic activity in northern Sulawesi (Walpersdorf *et al.* 1998). A continuous survey of the Palu Fault activity is of utmost importance, and the installation of permanent GPS sites in the Palu region is planned. Another permanent station is planned close to the earthquake-affected TOMI site. With the help of these observations we will be able to distinguish between transient and secular motions and thus constrain the modelling of the Sula block motion.

ACKNOWLEDGMENTS

A large part of this work was carried out in the framework of the GEODYSSSEA project. We are grateful to the GEODYSSSEA team, especially to Jürgen Klotz and the teams of GFZ Potsdam, Germany, and BAKOSURTANAL, Cibinong, Java, for the data collection and the field support in eastern Indonesia. We thank the geologists of Irwan Bahar's team at GRDC Bandung for their help during the field reconnaissance and the installation of the Sulawesi densification sites. Many thanks to Gero Michel and Peter Wilson (GFZ) for their careful revision of this text.

REFERENCES

- Angermann, D., Becker, M., Simons, W. & Walpersdorf, A., 1998. The solutions of the European analysis centres, *GEODYSSSEA Final Report*, eds Wilson, P. & Michel, G.W., Commission of the European Community, EC contract CII*CT93-0337.
- Chamot-Rooke, N., Vigny, C., Walpersdorf, A., LePichon, X., Huchon, P. & C. Rangin, 1998. Sundaland motion detected from GEODYSSSEA GPS measurements, *GEODYSSSEA Final Report*, eds Wilson, P. & Michel, G.W., Commission of the European Community, EC contract CII*CT93-0337.
- DeMets, C., Gordon, R.G., Argus, D.F. & Stein, S., 1994. Effect of recent revisions to the geomagnetic reversal time scale on estimates of current plate motions, *Geophys. Res. Lett.*, **21** (20), 2191–2194.
- Dong, D., 1993. The horizontal velocity field in Southern California from a combination of terrestrial and space-geodetic data, Massachusetts Institute of Technology, Cambridge, MA.
- Dong, D. & Bock, Y., 1989. Global Positioning System network analysis with phase ambiguity resolution applied to crustal deformation studies in California, *J. geophys. Res.*, **94**, 3949–3966.
- Feigl, K.L., King, R.W. & Jordan, T.H., 1990. Geodetic measurements of tectonic deformation in the Santa Maria fold and thrust belt, *J. geophys. Res.*, **95**, 2679–2699.
- Genrich, J.F., Bock, Y., McCaffrey, R., Calais, E., Stevens, C. & Subarya, C., 1996. Accretion of the southern Banda arc to the Australian plate margin determined by Global Positioning System measurement, *Tectonics*, **15**, 288–295.
- Hall, R., Nichols, G., Ballantyne, P., Charlton, T. & Ali, J., 1991. The character and significance of basement rocks of the southern Molucca Sea region, *J. SE Asian Earth Sci.*, **6**, 249–258.
- Herring, T.A., Davis, J.L. & Shapiro, I.I., 1990. Geodesy by radio interferometry: the application of Kalman filtering to the analysis of very long baseline interferometry data, *J. geophys. Res.*, **95**, 12 561–12 581.
- King, R.W. & Bock, Y., 1993. *Documentation for the MIT GPS Analysis Software: GAMIT*, Massachusetts Institute of Technology, Cambridge, MA.
- McCaffrey, R. & Abers, G.A., 1991. Orogeny in arc-continent collision: the Banda Arc and western New Guinea, *Geology*, **19**, 563–566.
- McCaffrey, R., Fauzi, Masturyono, Stevens, C., Nabelek, J., Schurr, B., Bock, Y., Subarya, C. & Puntodewo, T., 1996. Aftershock and GPS study of $M=8.2$ Biak earthquake of February 17, 1996, <http://gretchen.geo.rpi.edu/robmcc/biak.htm>.
- Moore, G.F. & Silver, E.A., 1983. Collision processes in the Northern Molucca Sea, in *The Tectonic and Geologic Evolution of Southeast Asian Seas and Islands*, Vol. 2, pp. 360–372, ed. Hayes, D.E., Geophys. Monogr., AGU.
- Peltzer, G. & Saucier, F., 1996. Present-day kinematics of Asia derived from geologic fault rates, *J. geophys. Res.*, **101**, 27 943–27 956.
- Puntodewo, S.S.O. *et al.*, 1994. GPS measurements of crustal deformation within the Pacific-Australia plate boundary zone in Irian Jaya, Indonesia, *Tectonophysics*, **237**, 141–153.
- Rangin, C., 1989. The Sulu Sea, a back-arc basin setting within a Neogene collision zone, *Tectonophysics*, **161**, 119–141.
- Rangin, C., Jolivet, L., Pubellier, M. & the Tethys Pacific Working Group, 1990. A simple model for the tectonic evolution of southeast Asia and Indonesia region for the past 43 m.y., *Bull. Soc. géol. Fr.*, **6**, 889–905.
- Rangin, C., Maury, R.C., Polvé, M., Bellon, H., Priadi, B., Soeria-Atmadja, R., Cotten, J. & Joron, J.-L., 1997. Eocene to Miocene back-arc basin basalts and associated island arc tholeiites from Northern Sulawesi (Indonesia): implications for the geodynamic evolution of the Celebes basin, *Bull. Soc. géol. France*, **168**, 627–635.
- Rangin, C., Pubellier, M., Chamot-Rooke, N., Walpersdorf, A., Vigny, C., LePichon, X., Aurelio, M. & Quebral, R., 1998. Quantitative estimation of plate convergence across the Sundaland/Philippine Sea plate boundary from GPS results (GEODYSSSEA), *Geophys. J. Int.*, submitted.

- Rothacher, M. & Mader, G., 1996. Combination of antenna phase center offsets and variations, *Antenna Calibration set IGS_01*, IGS Central Bureau/University of Berne, Berne, Switzerland.
- Silver, E.A., McCaffrey, R. & Smith, R.B., 1983. Collision, rotation, and the initiation of subduction in the evolution of Sulawesi, Indonesia, *J. geophys. Res.*, **88**, 9407–9418.
- Stevens, C. *et al.*, 1998. GPS evidence for rapid rotation about a vertical axis in a collisional setting: the Palu fault of Sulawesi, Indonesia, *Geophys. Res. Lett.*, submitted.
- Surmont, J., Laj, C., Kissel, C., Rangin, C., Bellon, H., & Priadi, B., 1994. New paleomagnetic constraints on the Cenozoic tectonic evolution of the north arm of Sulawesi, Indonesia, *Earth planet. Sci. Lett.*, **121**, 629–638.
- Tregoning, P. *et al.*, 1994. First geodetic measurement of convergence across the Java trench, *Geophys. Res. Lett.*, **21**, 2135–2138.
- Walpersdorf, A., Vigny, C., Subarya, C. & Manurung, P., 1998. Monitoring of the Palu-Koro fault by GPS, *Geophys. Res. Lett.*, **25** (13), 2313–2316.
- Wilson, P. & Rais, J., 1998. The GEODYSSSEA project: an investigation of the geology and geodynamics of South and South East Asia, *GEODYSSSEA Final Report*, eds Wilson, P. & Michel, G.W., Commission of the European Community, EC contract CII*CT93-0337.